Noname manuscript No.
(will be inserted by the editor)

Experimental validation of appropriate axial immersions for helical mills

Daniel Bachrathy · Jokin Munoa · Gabor Stepan

Received: date / Accepted: date

Abstract The forced periodic vibrations of milling processes with helical tools are modelled and analysed. By means of analytical and numerical techniques, the so-called superchart of milling is constructed that includes the conventional stability chart with the stability lobes and also the amplitudes of the stable forced vibrations, which is correlated to many surface quality numbers like surface location error, surface waviness, surface roughness. The existences of trivial and non-trivial appropriate axial immersions are presented for a single degree of freedom mechanical model of the machine tool structure. At these appropriate axial immersion parameters if the cutting is stable, the surface quality parameters will be also optimal even in those spindle speed domains where the system is near to resonance and the cutting efficiency is high. Experiments are performed with a large industrial milling machine using a flexible test rig with an essential flexibility in one direction. The calculated and the measured forced vibration signals in the stable domains of the stability chart are in good correlation, which validates the simple analytical predictions for the non-trivial appropriate axial immersion parameters.

D. Bachrathy
Department of Applied Mechanics, Budapest University of Technology and Economics, Budapest, H-1111, Hungary
Tel.: +36-1-463 1369
Fax: +36-1-463 3471
E-mail: bachrathy@mm.bme.hu

J. Munoa
Ideko-Ik4 Technological Centre, Elgoibar, Basque Country, Spain
E-mail: jmunoa@ideko.es

G. Stepan
Department of Applied Mechanics, Budapest University of Technology and Economics, Budapest, H-1111, Hungary
E-mail: stepan@mm.bme.hu

Keywords milling; chatter; machined surface quality; helical tool; appropriate axial immersion

1 Introduction

In milling processes, vibrations always occur due to the periodic material removal provided by the rotating milling tool which occasionally are combined with the so-called chatter originated in the possible instability of milling process. Using the terminology of vibration theory, the first kind of vibration is a so-called forced vibration, while the second is so-called self-excited vibration.

The essential limit for the increase of the material removal rate is the chatter caused by the surface regeneration effect [27,26,28]. The corresponding periodic, quasi-periodic or chaotic vibrations appear when the stationary milling loses its stability [23,25,24,8], in other words, when the stationary periodic forced vibrations becomes unstable. These types of vibrations destroy the surface integrity and can create heavy load on the machine tool. The so-called stability chart presents and predicts the chatter-free parameters domains of the milling process traditionally in the plane of the spindle speed and the axial immersion. In the parameter pockets between the so-called stability-lobes, large material removal rates can be reached while the milling is still chatter-free in spite of the fact that the corresponding spindle speeds lead to near-resonant forced vibrations [3,9,2]. The levels of the stable periodic forced vibrations are usually small and create negligible surface errors due to the high dynamic rigidity of the machine tool structure. However, large periodic forced vibrations are likely to occur just for the most efficient near-resonant spindle speeds, which are related to low

damping modes (for instance thin walls) [3,9,18,21,17, 7]. In these cases, the surface integrity is still given, but the maximal surface location error, the surface roughness and waviness may be large and intolerable [3]. These forced near-resonant vibrations also create an additional load on the machine tool. These problems result further limitation to the increase of the material removal rates, and the use of the cutting parameters in the efficient stable parameter pockets requires additional careful analysis.

In the paper [3], it is shown and proved analytically that both good surface properties and large material removal rate can be achieved by the application of the appropriate axial immersions in case of helical fluted tools even for resonant spindle speeds. The basic concept is that the resonant harmonic component of the cutting force that excites one of the natural frequencies of the system can be eliminated by using the so-called trivial and non-trivial appropriate axial immersions $a_{\mathrm{p}}^{\mathrm{app}}$ [3] are given by

$$a_{\mathrm{p}}^{\mathrm{app}} = jk\frac{p}{N}, \quad j = 0, 1, 2, 3, ... \tag{1}$$

$$a_{\mathrm{p}}^{\mathrm{app}} = j\frac{p\Omega}{\omega_n}, \quad j = 0, 1, 2, 3, ... \tag{2}$$

respectively, where N is the number of teeth of the milling tool, p is the helix pitch, Ω is the spindle speed and ω_n is the natural angular frequency of the system. The appropriate axial immersions determined by Eq. (1) are called trivial because the geometry and the kinematics of the milling process already explains clearly, why the resultant of the cutting forces does not vary in time; this is also well known for technologists.

Our goal is to verify the non-trivial appropriate axial immersions given in Eq. (2) by measurements via constructing an experimental superchart, which is the combination of the traditional stability chart and some surface quality parameters directly related to the forced vibration amplitudes [3,17,20].

Although, these simple formulae of the appropriate axial immersions are derived for SDoF systems, where either the tool or the workpiece is flexible, the results could be easily extended to multi-degree-of-freedom systems if the resonant spindle speeds are isolated [4].

2 Experimental setup and mechanical modelling

The measurements are performed with a large industrial milling machine (Soraluce SV-6000) on which a test rig is mounted with an essential flexibility in y direction (see Fig. 1). The experimental modal analysis performed by impact tests shows that the system has only one dominant vibration mode, indeed. The verified modal parameters like the natural angular frequency ω_n and the damping ratio ξ are presented in Table 1. With the help of the measured mass m of the test rig and the workpiece, all the mechanical parameters were identified including the stiffness k in y direction and also the corresponding damping factor c. Modal measurements implied, that the tool and the tool holder together with the whole machine tool structure are rigid relative to the workpiece holder.

Figure 2 shows a one degree of freedom (DoF) mechanical model of the milling process, where the param-

m [kg]	c [Ns/m]	k [N/μm]
132	974.24	43.89

$\omega_n = \sqrt{k/m}$	$\xi = c/(2m\omega_n)$
576.6 [rad/s] = 91.77 [Hz]	64%

Table 1 Measured modal parameters.

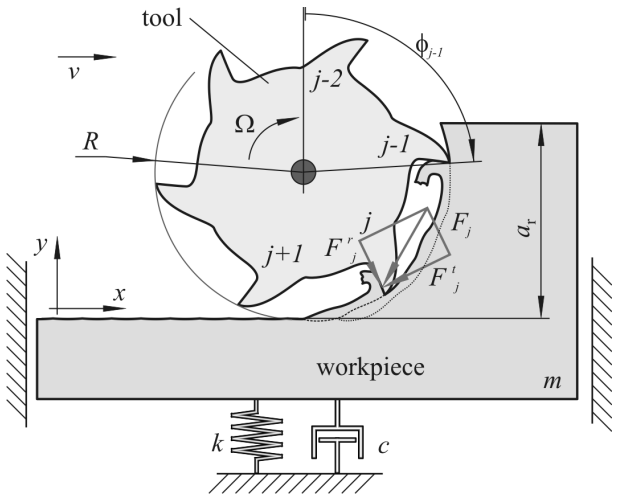

Fig. 2 One degree of freedom model of the milling process.

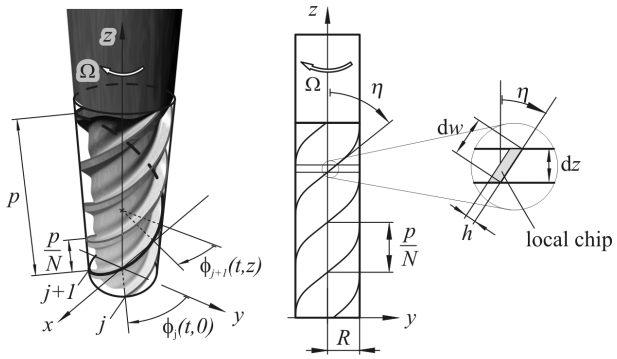

Fig. 3 Helix pitch p and angular position of the jth edge $\phi_j(t,z)$ as a function of the time t and the axial coordinate z [3].

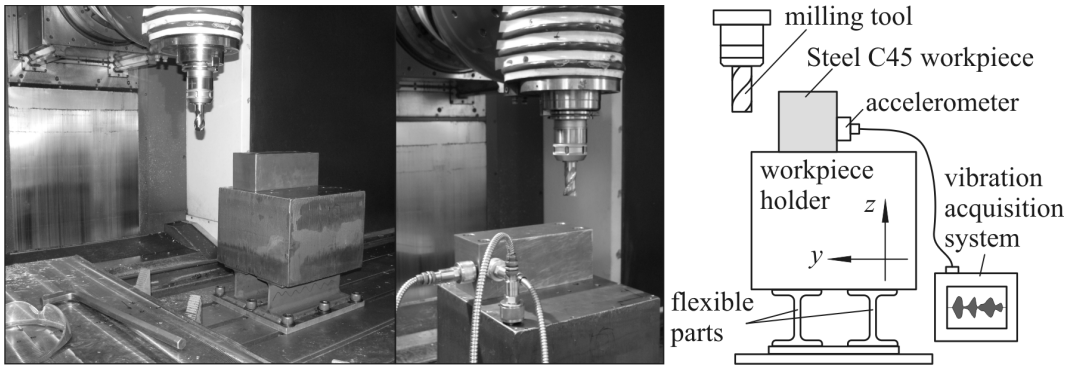

Fig. 1 Measurement setup: test rig flexible in y direction.

eters m, k and c correspond to the ones of the modal testing of the experimental rig. The system is excited by the resultant cutting force F. The governing equation of the workpiece motion is

$$m\ddot{y}(t) + c\dot{y}(t) + ky(t) = F(t). \tag{3}$$

The angular position of the jth helical cutting edge depends on the z coordinate that is parallel to the axis of the milling tool (see Fig. 3):

$$\phi_j(t,z) = t\Omega - j2\pi/N - \frac{2\pi z}{p}, \tag{4}$$

where Ω is the angular velocity of the milling tool, N is the number of flutes. The helix pitch p can be calculated from the helix angle η as follows:

$$p = \frac{2\pi R}{\arctan(\eta)}, \tag{5}$$

where R is the radius of the tool. In a cross section of infinitesimal width dz at the height z, the y component of the infinitesimal resultant cutting force is calculated by using the force model presented in [15,22] and [7]:

$$\begin{aligned} \mathrm{d}F = &\sum_{j=1}^{N} g(\phi_j(t,z)) \left(k_{0\mathrm{r}} \cos(\phi_j(t,z)) - k_{0\mathrm{t}} \sin(\phi_j(t,z))\right) \\ &+ h(t,z,y(t),y(t-\tau)) \\ &\times \left(k_{1\mathrm{r}} \cos(\phi_j(t,z)) - k_{1\mathrm{t}} \sin(\phi_j(t,z))\right) \mathrm{d}z \end{aligned} \tag{6}$$

where $k_{0\mathrm{r}}$ and $k_{0\mathrm{t}}$ are the specific edge coefficients, $k_{1\mathrm{r}}$ and $k_{1\mathrm{t}}$ are the specific shear force coefficients in the radial and the tangential direction, respectively. Considering the surface regenerative effect [23,9,18,17,10], the instantaneous chip thickness h at height z and at time instant t is given by

$$\begin{aligned} h(t,z,y(t),y(t-\tau)) = &f_z \sin(\phi_j(t,z)) \\ &+ (y(t-\tau) - y(t)) \cos(\phi_j(t,z)), \end{aligned} \tag{7}$$

where the time delay τ is just equal to the tooth pass period, and f_z is the feed per tooth. The screen function $g(\phi_j(t,z))$ indicates the contact between the segment of the cutting edge and the material, so it is 1 in the cutting phase, while it is 0 for the non-cutting phase [10,16]:

$$g(\phi_j(t,z)) = \begin{cases} 1 & \text{if } \phi_{\mathrm{enter}} < \phi_j(t,z) < \phi_{\mathrm{exit}}, \\ 0 & \text{otherwise}, \end{cases} \tag{8}$$

where the constant parameters ϕ_{enter} and ϕ_{exit} are the angles where the jth tooth enters and exits the workpiece material. Note, that the above defined screen function assumes a certain approximation when it neglects its dependence on $y(t)$ and $y(t-\tau)$, which would lead to state-dependent delay models as discussed in details in [5]. The resultant cutting force acting on the workpiece can be calculated by the integration of Eq. (6) with respect to z from zero to the axial immersion a_{p}. Accordingly, the cutting force can be expressed in the form

$$F(t,y(t),y(t-\tau)) = F_{\mathrm{stat}}(t) + \hat{w}\left(y(t-\tau) - y(t)\right), \tag{9}$$

where the stationary time-periodic component of the resultant cutting force is

$$\begin{aligned} F_{\mathrm{stat}}(t) = &\sum_{j=1}^{N} \int_0^{a_{\mathrm{p}}} g(\phi_j(t,z)) \\ &\Big(\left(k_{0\mathrm{r}} \cos(\phi_j(t,z)) - k_{0\mathrm{t}} \sin(\phi_j(t,z))\right) \\ &+ f_z \sin(\phi_j(t,z)) \left(k_{1\mathrm{r}} \cos(\phi_j(t,z)) - k_{1\mathrm{t}} \sin(\phi_j(t,z))\right) \Big) \mathrm{d}z \end{aligned} \tag{10}$$

and the time-periodic directional factor is defined by

$$\hat{w}(t) = \sum_{j=1}^{N} \int_0^{a_\mathrm{p}} g(\phi_j(t,z)) cos\phi_j(t,z)) \left(k_{1\mathrm{r}} \cos(\phi_j(t,z)) - k_{1\mathrm{t}} \sin(\phi_j(t,z))\right) \mathrm{d}z. \quad (11)$$

The combination of the above Eqs. (3,9,10,11) leads to the governing equation.

$$m\ddot{y}(t) + c\dot{y}(t) + (k + \hat{w})y(t) = F_{\mathrm{stat}}(t) + \hat{w}y(t-\tau). \quad (12)$$

This is a linear periodically forced delay-differential equation with time periodic coefficients, where the time delay, the time period of the forcing and the time period of the coefficients are the same. This way, Eq. (12) describes both the periodic forced vibration of the milling process and also its stability against possible chatter.

3 Forced vibration and its stability

The local motion of the workpiece is the linear combination of the periodic (chatter-free) forced vibration $y_\mathrm{p}(t)$ (also called particular solution) and the perturbed free vibration $y_\mathrm{h}(t)$ (also called homogeneous solution) that corresponds to the diminishing transient vibration in case of chatter-free parameters or to the exponentially increasing machine tool chatter in case of unstable machining process parameters:

$$y(t) = y_\mathrm{p}(t) + y_\mathrm{h}(t). \quad (13)$$

The periodic forced vibration satisfies the ordinary differential equation

$$m\ddot{y}_\mathrm{p}(t) + c\dot{y}_\mathrm{p}(t) + ky_\mathrm{p}(t) = F_{\mathrm{stat}}(t), \quad (14)$$

since the delayed terms are cancelled due to the equality of the delay and the periodicity [9]. Combining Eqs. (12), (13) and (14), the governing equation of the perturbed free vibration is given by

$$m\ddot{y}_\mathrm{h}(t) + c\dot{y}_\mathrm{h}(t) + (k + \hat{w})y_\mathrm{h}(t) = \hat{w}y(t-\tau). \quad (15)$$

This time-periodic delay-differential equation describes the stability of the stationary workipece motion $y_\mathrm{p}(t)$. This linear stability is examined by the so-called semi-discretization method developed, described and tested by Insperger and Stepan [11,12,14,6,30,13].

The periodic solution of the workpiece motion is calculated in the frequency domain [3,7]

$$\mathscr{F}\left(y_\mathrm{p}\right)(\omega) = \frac{\mathscr{F}\left(F_{\mathrm{stat}}\right)(\omega)}{-\omega^2 m + \mathrm{i}\omega c + k}, \quad (16)$$

where $\mathscr{F}$ refers to the Fourier transformation. In our numerical algorithm, the stationary force function in the frequency domain was calculated by the Matlab built-in Fast Fourier Transformation (fft) and the Inverse Fast Fourier Transform (ifft) was used to determine the periodic motion of the workpiece in the time domain. Instead of evaluating the integration with respect to z in Eqs. (10) and (11), a finite sum was used with sufficiently small integration steps of size about 2 [μm]. During the calculations, the modal parameters of the experimental setup were used (see Table 1 in Section 2).

4 Results and experimental validation

In the test case and in the experiments, a two fluted helical cutting tool (N=2) was used with 30 [mm] diameter, 42° helix angle and p=104.67 [mm] helix pitch (Garant 191100 STG 104.67 NC HSS-Co8). The machined material was Steel C45 and its corresponding cutting coefficients (see Table 2) were measured based on a method explained in details in [19,29,1].

$k_{1\mathrm{t}}$ [N/mm^2]	$k_{1\mathrm{r}}$ [N/mm^2]	$k_{0\mathrm{t}}$ [N/mm]]	$k_{0\mathrm{r}}$[N/mm]
1697	476	58	37

Table 2 Specific cutting coefficients.

During the measurements, constant feed per tooth $f_z = \tau v = 0.15$ [mm/tooth] was used with radial immersion a_r=0.75 [mm] ($a_\mathrm{r}/D = 2.5\%$) in down-milling operation. Accordingly, the enter and exit angles are $\phi_{\mathrm{enter}} = 161.805°$ and $\phi_{\mathrm{exit}} = 180°$, respectively. It is important to note, that the appropriate axial immersion values are independent from the radial immersion, feed rate and even from the force function characteristics. This means, that even if a nonlinear cutting force characteristics with different radial immersion and feed rate values would be applied, the appropriate axial immersion values would be the same, however, the stability properties could be different.

Our goal was to verify the non-trivial appropriate axial immersion values (see. Eq.(2)). Accordingly, the experiments were carried out at the first three resonant spindle speeds $n = \Omega 60/(2\pi)$=2775, 1387, 925 [rpm], at a non-resonant one n=2500 [rpm], and for a set of five axial immersions a_p=43.6, 34.9, 26.1, 17.4, 8.7 [mm]. These cutting parameters are denoted by circles in the superchart of Fig. 4 that represents both the stability chart and the forced vibration amplitudes in the stable parameter domains [3,17,20].

In this figure, the trivial appropriate axial immersions given by Eq. (1) and the non-trivial ones given by Eq. (2) are denoted by horizontal dotted lines and

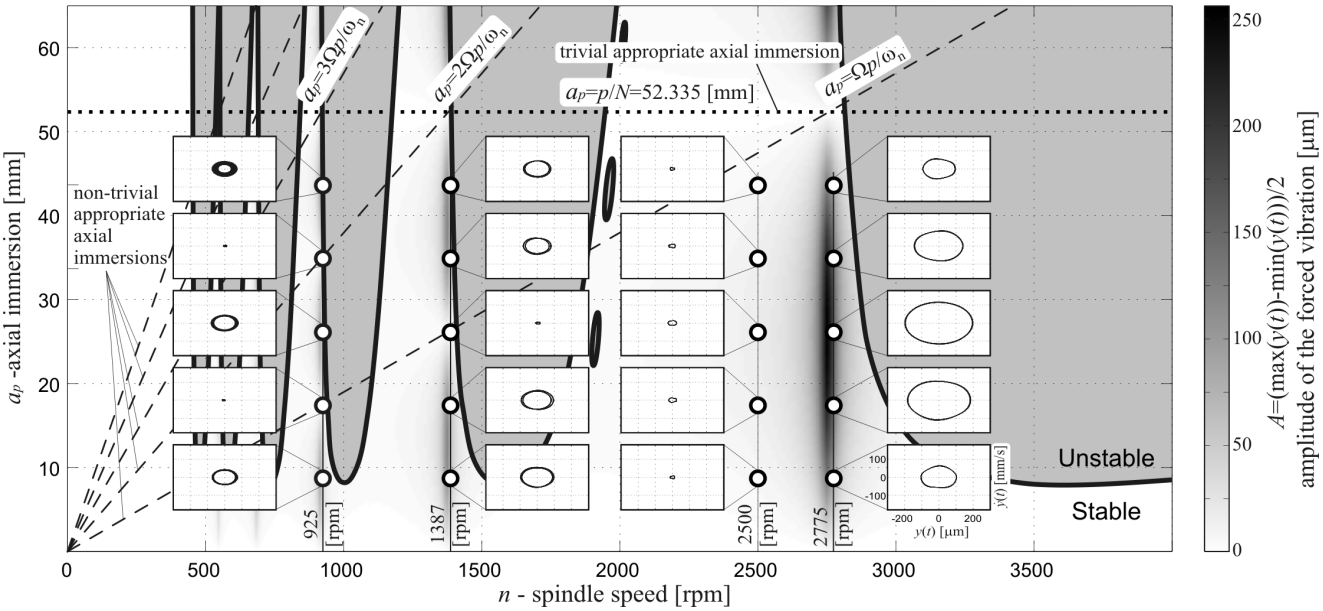

Fig. 4 Superchart of milling. Calculated dark gray regions (lobes) refer to chatter (unstable stationary milling). Calculated amplitudes of the forced vibrations are presented by gray scale in the stable domains (stable pockets between the lobes). Small panels present measured vibration in phase plane $(y, \dot{y})$ at the measurement parameters denoted by circles. A trivial appropriate axial immersions and non-trivial ones are denoted by a horizontal dotted lines and slanting dashed lines, respectively.

slanting dashed lines, respectively. During the experiments, the acceleration of the workpiece was measured by piezo accelerometers then the time signals were integrated twice numerically and filtered by high-pass filter at the cut off frequency 5Hz. The two dimensional projections of the (infinite dimensional) phase space to the plane $(y, \dot{y})$ of the measured signals are plotted in Fig. 5 after the transient motions died out. Note the non-uniform scales of the panels. The same panels show the corresponding calculated periodic forced vibrations, too, where the static deformation component is subtracted to be able to compare the results with the measured high-pass filtered signals. The same phase plots of the measured vibrations are inserted to the superchart of Fig. 4 where a uniform scale is used. This way, Fig. 4 presents a comparison of the measured and the theoretically predicted forced vibrations in the stable cutting parameter domains. Another representation of the measured data can be found in Fig. 6 where the measured and calculated amplitudes ($A = (\max_t(y(t)) - \min_t(y(t)))/2$) of the periodic forced vibrations are plotted for the selected spindle speeds denoted by continuous vertical thin lines in Fig. 4. All these representations in Figs. 4, 5 and 6 show that the measured vibration amplitudes are significantly smaller in the vicinity of the non-trivial appropriate axial immersions determined in Eq. (2), which provides an experimental validation of the theoretical predictions of [3].

5 Conclusion

In our theoretical approach, a one degree of freedom mechanical model of the milling process was presented for helical mills. The specific edge and shear force coefficients were applied in the cutting force function against the chip width. Based on the theory introduced in [3], the trivial and non-trivial appropriate axial immersions were calculated numerically. The corresponding horizontal and slanting parameter lines were presented in the superchart together with the classical stability-lobes and the forced vibration amplitudes in the chatter-free parameter domains. Experiments were carried out to validate the theoretically predicted non-trivial appropriate axial immersions. Good correlation was found between the measured and the calculated results, which validates the simple analytical formulas (2) obtained for the non-trivial appropriate axial immersions. Also, we measured smaller vibration amplitudes by setting the non-trivial appropriate axial immersion values in case of resonant spindle speeds, than the vibration amplitudes at any arbitrary axial immersion in case of a non-resonant spindle speed (compare, for example, the second and the third vertical lines in Fig. 4). Note, that even smaller forced vibrations can be achieved at non-resonant spindle speeds and at appropriate axial immersions, although the advantage of high efficiency between the stability lobes cannot be exploited in these cases. The main advantage of the application of non-trivial appropriate axial immersions is that the actual axial

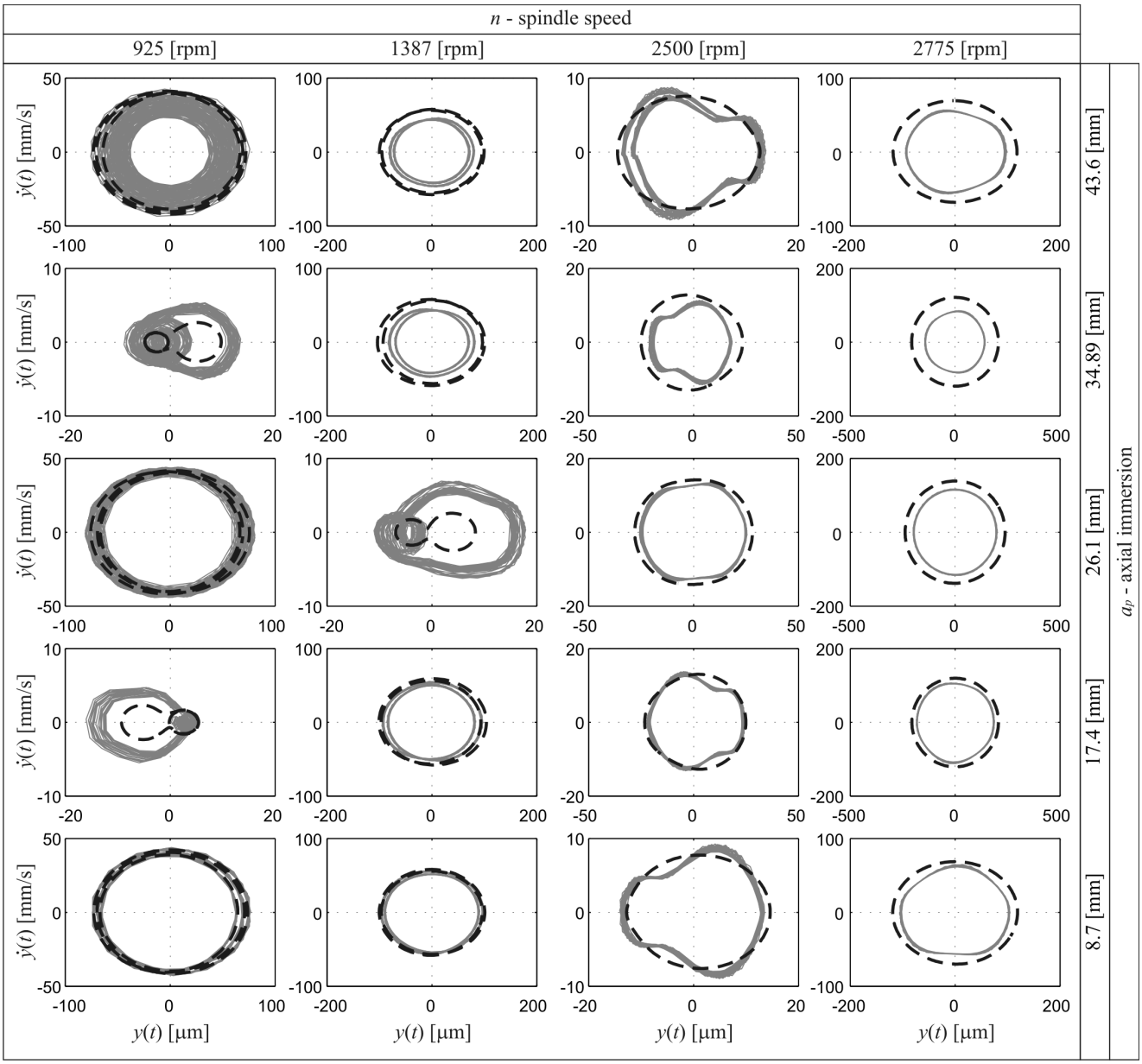

Fig. 5 Measured (gray continuous line) and calculated (dashed black line) phase plots of the forced periodic vibration of the workpiece. Note changes of scales!

immersion can be set to a much smaller value then the helix pitch, which is a trivial appropriate axial immersion. The trivial appropriate axial immersions (1) often cannot be applied due to certain limits of the machining process parameters, or simply due to the length of the milling tool as it was the case in our experiment series, too.

Acknowledgements The work was supported by the Jnos Bolyai Research Scholarship of the Hungarian Academy of Science and by the Hungarian Scientific Research Fund under grant OTKA PD112983 and K101714 and by EU FP7 HIP-POCAMP project (608800/ FP7-2013-NMP-ICT-FOF) The research leading to these results has received funding from the European Research Council under the European Unions Seventh Framework Programme (FP/2007-2013) / ERC Advanced Grant Agreement n. 340889.

References

1. Altintas, Y.: Manufacturing Automation: Metal Cutting Mechanics, Machine Tool Vibrations, and CNC Design. Cambridge university press (2012)
2. Bachrathy, D., Homer, M., Insperger, T.I., Stepan, G.: Surface location error for helical mills. In: 6th International Conference on High Speed Machining. San Sebastian, Spain, 03.21-03.22, Paper C100., pp. 379–384

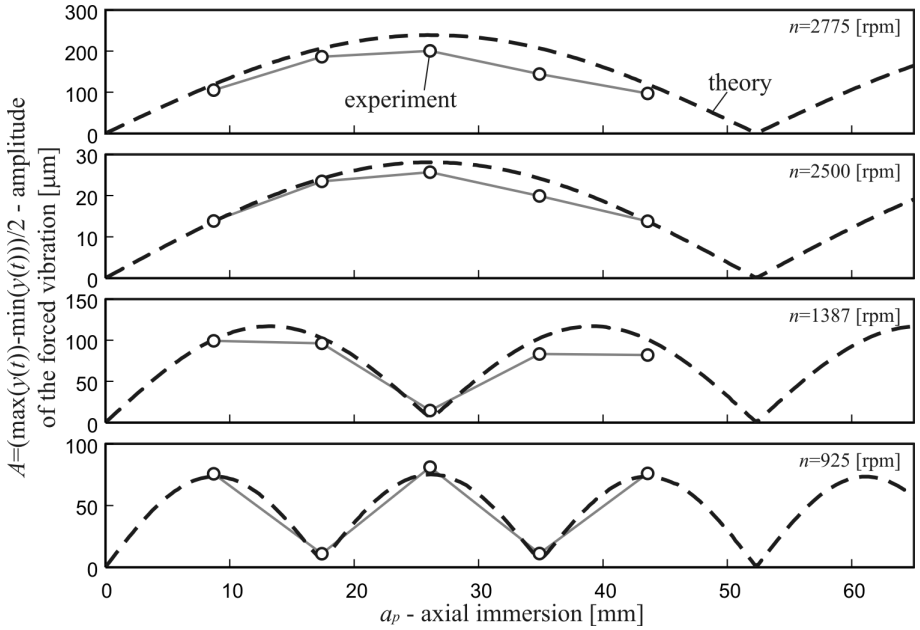

Fig. 6 Amplitudes of the measured and the calculated forced vibrations denoted by gray continuous lines and circles, and dashed black lines, respectively. Note changes of scales!

(2007). URL `http://mycite.omikk.bme.hu/doc/72136.pdf`

3. Bachrathy, D., Insperger, T., Stepan, G.: Surface properties of the machined workpiece for helical mills. Machining Science and Technology **13**(2), 227–245 (2009). URL `http://mycite.omikk.bme.hu/doc/73736.pdf`
4. Bachrathy, D., Stepan, G.: Optimal axial immersion for helical milling tools based on frequency response function (optimalis axialis fogasmelyseg csavart elu maroszerszamra frekvencia atviteli fuggveny alkalmazasaval (in hungarian). Gep **LXI**(9-10), 3–6 (2010). URL `http://mycite.omikk.bme.hu/doc/96781.pdf`
5. Bachrathy, D., Stepan, G.: State dependent regenerative effect in milling processes. In: Proceedings of the 7th European Nonlinear Dynamics Conference (ENOC 2011): Systems with Time Delay (MS-11). Rome, Italy, 07.24-07.29, MS11-21, ISBN: 978-88-906234-2-4, pp. 1–2 (2011). URL `http://marabu.omikk.bme.hu/doc/107421.pdf`
6. Balachandran, B., Kalmar-Nagy, T., Gilsinn, D.E.: Delay Differential Equations: Recent Advances and New Directions. Spinger (2009)
7. Cheng, K.: Machining dynamics: fundamentals, applications and practices. Springer Science & Business Media (2008)
8. Dombovari, Z., Wilson, R.E., Stepan, G.: Estimates of the bistable region in metal cutting. Proceedings of the Royal Society A: Mathematical, Physical and Engineering Sciences **464**(2100), 3255–3271 (2008)
9. Insperger, T., Gradisek, H., Kalveram, M., ad K. Weinert, G.S., Govekar, E.: Machine tool chatter and surface location error in milling processes. Journal of Manufacturing Science and Engineering **128**(4), 913–920 (2006)
10. Insperger, T., Stepan, G.: Stability of high-speed milling. In: Proceedings of ASME International Mechanical Engineering Congress and Exposition, 241, pp. 119–123. ASME, Orlando, Florida (2000)
11. Insperger, T., Stepan, G.: Semi-discretization of delayed dynamical systems. In: Proceedings of the ASME 2001 Design Engineering Technical Conferences, DETC2001/VIB-21446 (CD-ROM), p. 6. ASME, Pittsburgh, Pennsylvania (2001)
12. Insperger, T., Stepan, G.: Updated semi-discretization method for periodic delay-differential equations with discrete delay. International Journal of Numerical Methods in Engineering **61**(1), 117–141 (2004)
13. Insperger, T., Stepan, G.: Semi-Discretization for Time-Delay Systems, 1 edn. Applied Mathematical Sciences. Springer, 1 (2011)
14. Insperger, T., Stepan, G., Turi, J.: On the higher-order semi-discretizations for periodic delayed systems. Journal of Sound and Vibration **313**, 334–341 (2008)
15. Kline, W., Devor, R., Shareef, I.: Prediction of surface accuracy in end milling. ASME Journal of Engineering for Industry **104**, 272278 (1982)
16. Laczik, B.: Vibration monitoring of cutting processes. Ph.D. thesis, BME (1986)
17. Mann, B.P., Young, K.A., Schmitz, T.L., Diley, D.N.: Simultaneous stability and surface location error predictions in milling. Journal of Manufacturing Science and Engineering **127**, 446–453 (2005)
18. Montgomery, D., Altintas, Y.: Mechanism of cutting force and surface generation in dynamic milling. Journal of Engineering for Industry **113**, 160–168 (1991)
19. Munoa, J.: Desarrollo de un modelo general para la prediccion de la estabilidad del proceso de fresado. aplicacion al fresad periferico, al planeado convencional y a la caracterizacion de la estabilidad dinmica de fresadoras universales (in spanish). Ph.D. thesis, Mondragon University (2007)
20. Schmitz, T., Smith, K.S.: Machining Dynamics: Frequency Response to Improved Productivity. Springer, New York, NY (2009)
21. Shirase, K., Altintas, Y.: Cutting force and dimensional surface error generation in peripheral milling with variable pitch helical end mills. International Journal of Machine Tools and Manufacture **36**(6), 567–584 (1996)

22. Spence, A., Altintas, Y.: Cad assisted adaptive control for milling. ASME Journal of Dynamic Systems, Measurement and Control **113**, 444450 (1991)
23. Stepan, G.: Retarded Dynamical Systems. Longman, Harlow (1989)
24. Stepan, G., Szalai, R., Mann, B.P., Bayly, P.V., Insperger, T., Gradisek, J., Govekar, E.: Nonlinear dynamics of high-speed milling - analysis, numerics, and experiments. ASME Journal of Vibration and Acoustics **127**, 197–203 (2005)
25. Szalai, R., Stepan, G., Hogan, S.J.: Global dynamics of low immersion high-speed milling. Chaos **14**, 1069–1077 (2004)
26. Tlusty, J., Polacek, M.: The stability of machine-tool against self-excited vibration in machining. Proceedings of the International Research in Production Engineering, American Society of Mechanical Engineers (ASME) p. 465 (1963)
27. Tlusty, J., Spacek, L.: Self-excited vibrations on machine tools. Prague, Czech Republic: Nakl CSAV. [In Czech.] (1954)
28. Tobias, S.A.: Machine Tool Vibration. Blackie and Son, Ltd., London (1965)
29. Tobias, S.A., Fishwick, W.: The chatter of lathe tools under orthogonal cutting conditions. Trans. ASME **80**, 1079–1088 (1958)
30. Zatarain, M., Munoa, J., Peigne, G., Insperger, T.: Analysis of the influence of mill helix angle on chatter stability. CIRP Annals - Manufacturing Technology **55**(1), 365 – 368 (2006). DOI DOI:10.1016/S0007-8506(07)60436-3. URL http://www.sciencedirect.com/science/article/B8CXH-4P37B21-30/2/29db69aeaad8b206013925dd868271ba